Anal. Chem. **2009,** *81,* 4560–4565

Visualizing Quantum Dots in Biological Samples Using Silver Staining

Leo Y. T. Chou,[†] Hans C. Fischer,[†,‡] Steve D. Perrault,[†] and Warren C. W. Chan*[,†,‡]

Institute of Biomaterials & Biomedical Engineering, Donnelly Centre for Cellular and Biomolecular Research, and Department of Materials Science and Engineering, University of Toronto, Toronto, Ontario, Canada

Quantum dot (QD) based contrast agents are currently being developed as probes for bioimaging and as vehicles for drug delivery. The ability to detect QDs, regardless of fluorescence brightness, in cells, tissues, and organs is imperative to their development. Traditional methods used to visualize the distribution of QDs in biological samples mainly rely on fluorescence imaging, which does not account for optically degenerate QDs as a result of oxidative quenching within the biological environment. Here, we demonstrate the use of silver staining for directly visualizing the distribution of QDs within biological samples under bright field microscopy. This strategy involves silver deposition onto the surface of QDs upon reduction by hydroquinone, effectively amplifying the size of QDs until visible for detection. The method can be used to detect non-fluorescent QDs and is fast, simple, and inexpensive.

Recent advances in nano-based contrast agents for biomedical imaging applications have prompted investigations toward understanding their interactions with biological systems.[1−7] One such class of materials, semiconductor quantum dots (QDs), often rely on fluorescence imaging for visualizing their patterns of uptake and distribution within various biological systems. This approach, however, fails to account for optically degenerate QDs, either possibly as a result of oxidative quenching[8] or enzymatic degradation,[9] within the biological sample of interest (e.g., cells and tissues), as well as within archival specimens. Substantial loss in fluorescence signals is further compromised by variable increases in background levels associated with the process of specimen embedding and fixation.[10] While non-optical modalities such as electron microscopy are often used, they require additional sample processing steps, are limited to small field-of-views, and are relatively expensive.

Here, we propose a facile strategy for visualizing a precise histological landscape of QDs in biological tissues using a silver staining approach, in which QDs are grown into silver clusters of dimensions visible under direct light microscopy. In the past, silver staining methods have been extensively employed in gel electrophoresis,[11] to enhance visibility of metallic probes in immunolabeling,[12] and tracing of exogenous and endogenous metal ions in biological tissues.[13] In this study, we demonstrate specific localization of CdSe/ZnS core-shell nanocrystals, the most commonly studied QDs for biomedical applications to-date, within formalin-treated, paraffin-embedded (FFPE) tissue sections using silver staining reagents (Ag+, hydroquinone). We show excellent co-localization between silver stains and QDs and that this general technique can be employed to circumvent the aforementioned complications associated with fluorescence and electron microscopy. Of practical importance, we have found this mechanism to be robust in staining QDs of varying surface compositions (CdSe, CdS, ZnS) and with different polymer coatings such as poly(ethylene glycol) (PEG) and poly(acrylic acid) modified octadecylamine (PAA-ODA).

EXPERIMENTAL SECTION

Reagents. Silver staining solution (silver nitrate ($AgNO_3$) and hydroquinone) was obtained from Ted Pella Inc. Cadmium nitrate ($Cd(NO_3)_2$), phosphate buffered saline (PBS), and fetal bovine serum (FBS) were obtained from Sigma-Aldrich; 0.5 μm polystyrene beads were obtained from Bangs Laboratories Inc. Sodium hypochlorite (NaOCl, 15%) was purchased from Bioshop Inc. Hypochlorous acid solution (HOCl) was prepared fresh before use by dilution of NaOCl with Millipore nanopure water.

* To whom correspondence should be addressed. E-mail: warren.chan@utoronto.ca.

[†] Institute of Biomaterials & Biomedical Engineering.

[‡] Department of Materials Science and Engineering.

(1) Fischer, H. C.; Chan, W. C. W. *Curr. Opin. Biotechnol.* **2007**, *18*, 565–571.

(2) Fischer, H. C.; Liu, L.; Pang, K. S.; Chan, W. C. W. *Adv. Funct. Mater.* **2006**, *16*, 1299–1305.

(3) Gao, X.; Cui, Y.; Levenson, R. M.; Chung, L. W.; Nie, S. *Nat. Biotechnol.* **2004**, *22*, 969–976.

(4) Huh, Y. M.; Jun, Y. W.; Song, H. T.; Kim, S.; Choi, J. S.; Lee, J. H.; Yoon, S.; Kim, K. S.; Shin, J. S.; Suh, J. S.; Cheon, J. *J. Am. Chem. Soc.* **2005**, *127*, 12387–12391.

(5) Kim, S.; Lim, Y. T.; Soltesz, E. G.; De Grand, A. M.; Lee, J.; Nakayama, A.; Parker, J. A.; Mihaljevic, T.; Laurence, R. G.; Dor, D. M.; Cohn, L. H.; Bawendi, M. G.; Frangioni, J. V. *Nat. Biotechnol.* **2004**, *22*, 93–97.

(6) Sanhai, W. R.; Sakamoto, J. H.; Canady, R.; Ferrari, M. *Nat. Nanotechnol.* **2008**, *3*, 242–244.

(7) Singh, R.; Pantarotto, D.; Lacerda, L.; Pastorin, G.; Klumpp, C.; Prato, M.; Bianco, A.; Kostarelos, K. *Proc. Natl. Acad. Sci. U.S.A.* **2006**, *103*, 3357–3362.

(8) Mancini, M. C.; Kairdolf, B. A.; Smith, A. M.; Nie, S. *J. Am. Chem. Soc.* **2008**, *130*, 10836–10837.

(9) Lovric, J.; Cho, S. J.; Winnik, F. M.; Maysinger, D. *Chem. Biol.* **2005**, *12*, 1227–1234.

(10) Del Castillo, P.; Llorente, A. R.; Stockert, J. C. *Basic Appl. Histochem.* **1989**, *33*, 251–257.

(11) Bassam, B. J.; Caetano-Anolles, G.; Gresshoff, P. M. *Anal. Biochem.* **1991**, *196*, 80–83.

(12) Holgate, C. S.; Jackson, P.; Cowen, P. N.; Bird, C. C. *J. Histochem. Cytochem.* **1983**, *31*, 938–944.

(13) Danscher, G.; Stoltenberg, M. *Prog. Histochem. Cytochem.* **2006**, *41*, 57–139.

10.1021/ac900344a CCC: $40.75
Published on Web 05/01/2009

Table 1. Summary of the Size, Surface Chemistry, and Optical Properties of Semiconductor QDs Used in This Work[a]

surface coating	approx. core diameter (nm)	approx. hydrodynamic diameter (nm)	fluorescence peak (nm, in H_2O)	fwhm (nm, in H_2O)
PAA-ODA	4.9	29	607	30
PEG	3.2	79	558	26
Ly-MUA	5.5	25	619	25
BSA	5.5	80	619	25

[a] The chemical composition of all QDs consisted of a CdSe-core capped with ZnS. Core diameter was estimated by sizing curves from Yu et al.[18] Hydrodynamic diameter was measured by dynamic light scattering (Malvern Particle Size Analyzer).

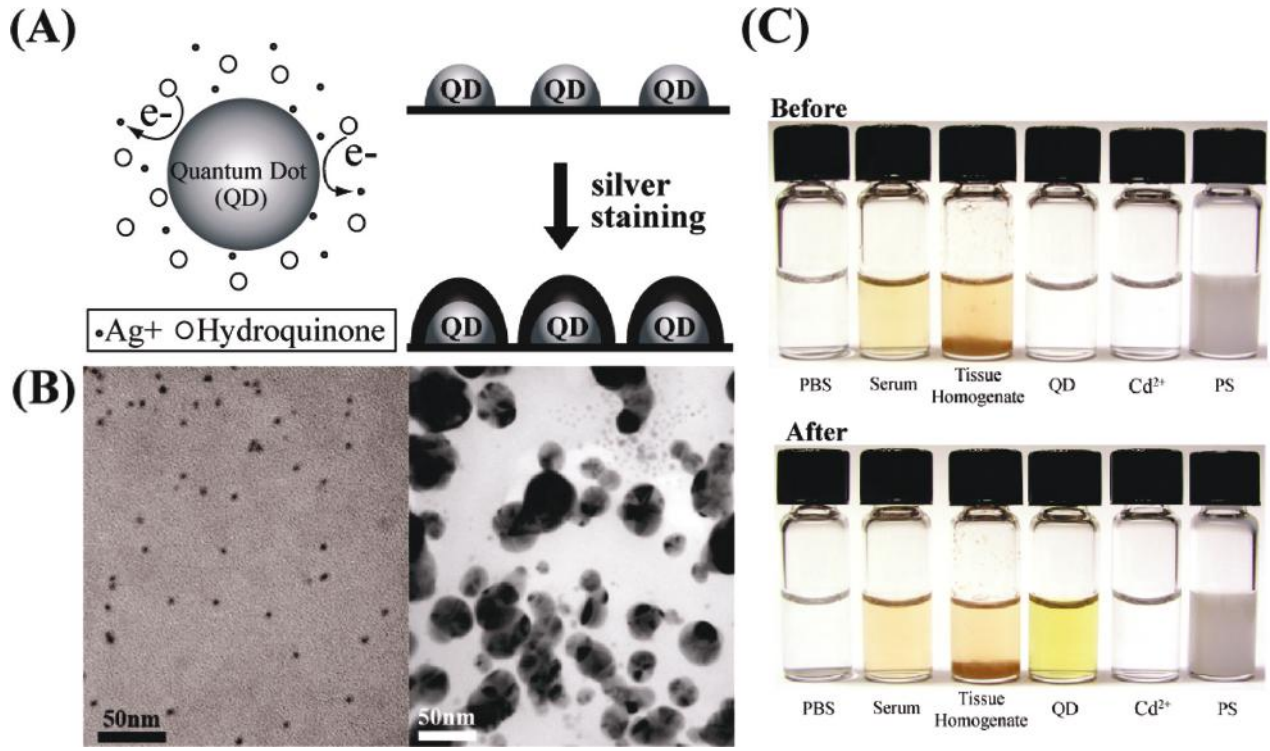

Figure 1. Silver staining of semiconductor QDs. (A) Schematic diagram depicting the mechanism of the silver staining process. (B) TEM image of PAA-ODA coated CdSe/ZnS QDs before (left) and after (right) silver growth. (C) Colorimetric response of different solutions to silver reduction. Note the darker color of QD solution after silver staining. PBS: phosphate buffered saline; PS: polystyrene beads.

QD Synthesis and Solubilization. ZnS-capped CdSe QDs with trioctylphosphine oxide (TOPO) or trioctylphosphine oxide-hexadecylamine (TOPO/HDA) as organic ligands were synthesized following published methods[14,15] and stored in chloroform until use. Various types of water-soluble QDs were prepared (PEG, PAA-ODA, or lysine-cross-linked mercaptoundecanoic acid (Ly-MUA)) according to previously published procedures.[2,16] The size, surface chemistry, and optical properties of QDs used in this work are summarized in Table 1.

Silver Deposition on QDs. For this proof-of-concept study, 10 μL of silver staining solution (1:1 $AgNO_3$/hydroquinone) was added to 100 nM solution of PAA-ODA encapsulated QDs in borate buffer (50 mM, pH 8.5). Formation of silver particles was monitored by visual inspection and by transmission electron microscopy (TEM). For TEM, QD solution was deposited onto copper grids (Carbon type B 300, Ted Pella Inc.) until dry followed by deposition of silver staining solution and rinsing with Millipore Nanopure water. To compare the catalytic potential of QD surface versus other materials, we examined the colorimetric response of PBS, tissue homogenate, FBS, $Cd(NO)_3$, and polystyrene beads upon exposure to the silver staining solution.

Oxidative Quenching of QDs and Detection with Silver Staining. PAA-ODA encapsulated QDs were diluted to a final concentration of 100 nM into borate buffer (50 mM, pH8.5) with 0−1000 μM of HOCl present. Changes in photoluminescence intensity of QDs upon exposure to HOCl were measured by Fluoromax 3 spectrofluorometer, and the integrity of the QDs was monitored by UV−vis absorbance using Shimadzu 2401 PC spectrophotometer. For silver staining, 10 μL of silver staining solution (1:1 $AgNO_3$/hydroquinone) was added to the QD solution. Formation of silver nanoparticles was confirmed by observing silver absorbance peak at 400 nm.

Silver Staining of QDs in Biological Samples. Silver staining of QDs in biological tissues were demonstrated on FFPE sections

(14) Hines, M. A.; Guyot-Sionnest, P. *J. Phys. Chem.* **1996**, *100*, 468–471.
(15) Dabbousi, B. O.; RodriguezViejo, J.; Mikulec, F. V.; Heine, J. R.; Mattoussi, H.; Ober, R.; Jensen, K. F.; Bawendi, M. G. *J. Phys. Chem. B* **1997**, *101*, 9463–9475.
(16) Anderson, R. E.; Chan, W. C. W. *ACS Nano* **2008**, *2*, 1341–1352.
(17) Danscher, G.; Howell, G.; Perezclausell, J.; Hertel, N. *Histochemistry* **1985**, *83*, 419–422.
(18) Yu, W. W.; Qu, L. H.; Guo, W. Z.; Peng, X. G. *Chem. Mater.* **2003**, *15*, 2854–2860.

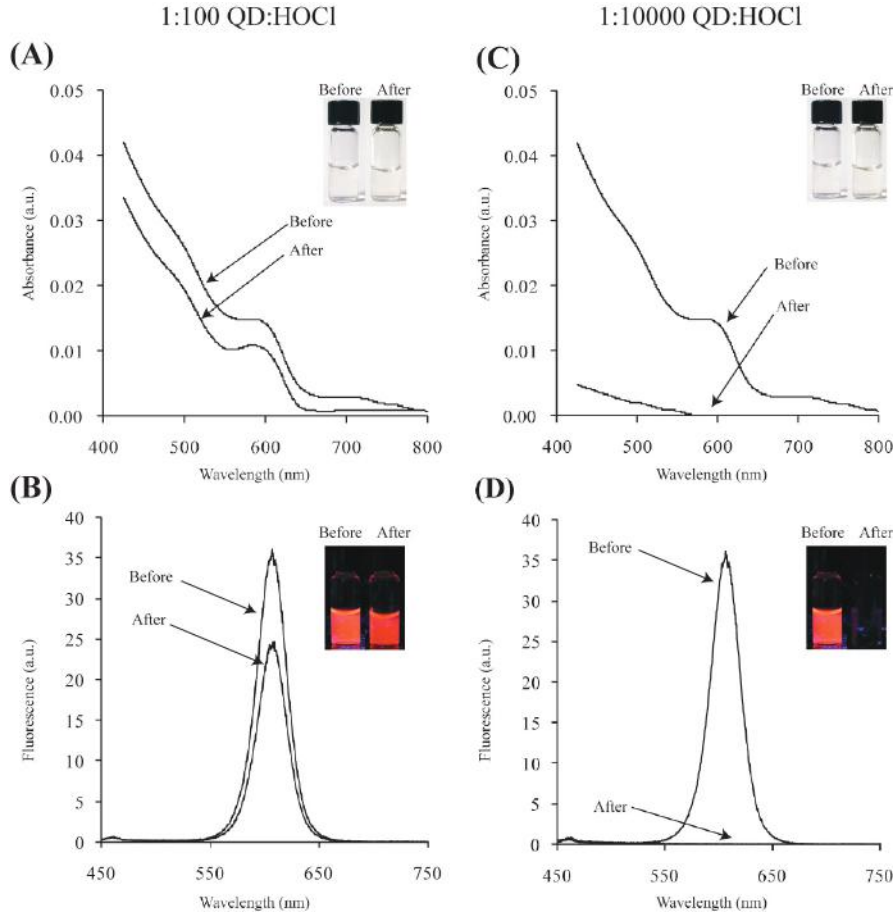

Figure 2. Oxidative quenching of PAA-ODA coated QDs using hypochlorous acid (HOCl). PAA-ODA coated QDs were diluted to 100 nM and mixed with 10 μM or 1000 μM HOCl in borate buffer (0.05 M, pH 8.5) at room temperature for 5 min. (A, B) At a molar ratio of 1:100 QD/HOCl, considerable fluorescence quenching was observed before significant changes in UV−vis absorbance, indicating the presence of localized surface defects on the QDs. (C, D) At a molar ratio of 1:10000, significant chemical dissolution of QDs was observed, as indicated by loss of both UV−vis absorbance and photoluminescence.[8]

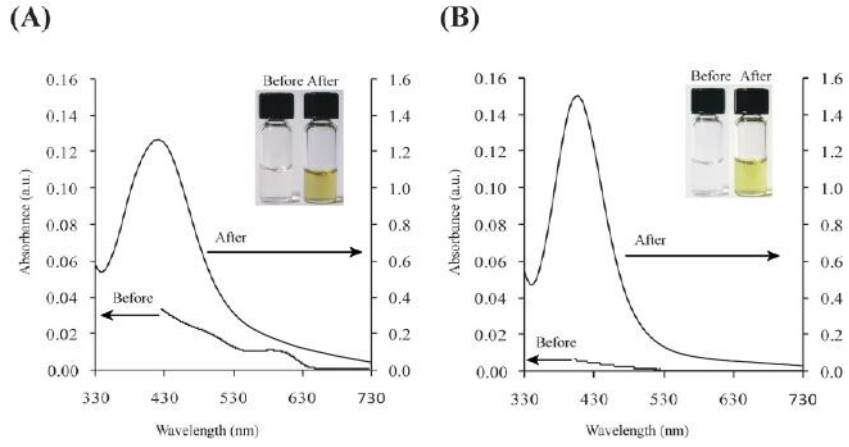

Figure 3. Silver staining of optically degenerate QDs as a result of oxidative quenching. QDs with either (A) localized surface defects or (B) chemical dissolution were silver stained as monitored by an absorbance peak at ~400 nm.

of rat lymph node tissues and liver tissues containing Ly-MUA QDs and PEG-QDs, respectively. In a typical experiment, FFPE sections were dewaxed, cleaned with deionized water for 30 s, and exposed to aliquots of the silver staining mixture for 45 to 80 min. Staining was terminated by rinsing the tissue sections under superfluous amounts of deionized water for up to 30 s. Blank tissue sections were similarly stained as negative control.

RESULTS AND DISCUSSION

Depicted in Figure 1A, the mechanism of silver staining rests on the ability of metallic, or in this case, semiconducting nanostructures, to coordinate electron transfer between silver ions and a reducing agent (e.g., hydroquinone) adhering to its surface. When silver ions and hydroquinone diffuse through a tissue section containing such catalytic nanostructures, both silver ions

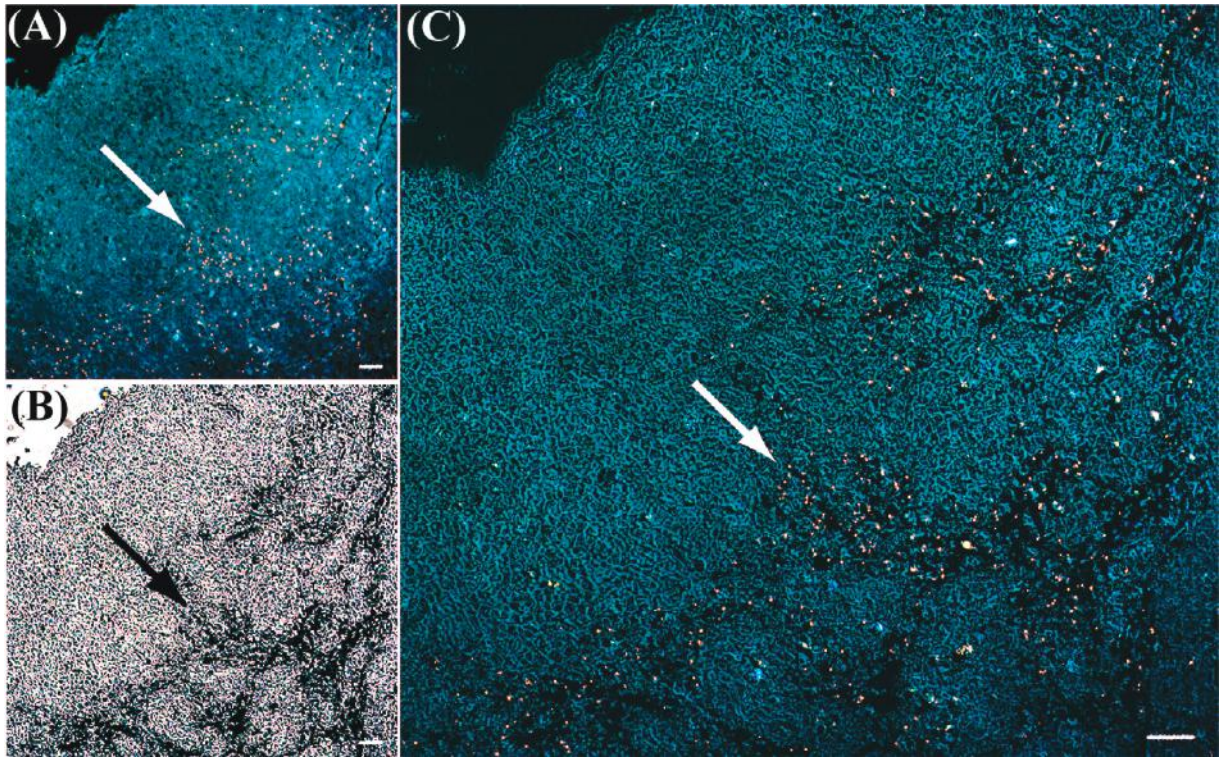

Figure 4. Histological images of a rat lymph tissue demonstrating QD-specific silver staining. (A) Fluorescence image of Ly-MUA QDs localized in rat tissue. (B) QDs were visualized as black grains under optical microscopy after silver staining. (C) An overlay of fluorescence image on bright-field image demonstrates excellent co-localization (see arrows) between the QD distribution pattern and the silver grains (C). Scale bars are 20 μm. Fluorescence image taken with Olympus IX71 inverted epifluorescence microscope ($\lambda_{Excitation}$ = 360/40 nm, $\lambda_{Emission}$ = 430 nm long pass).

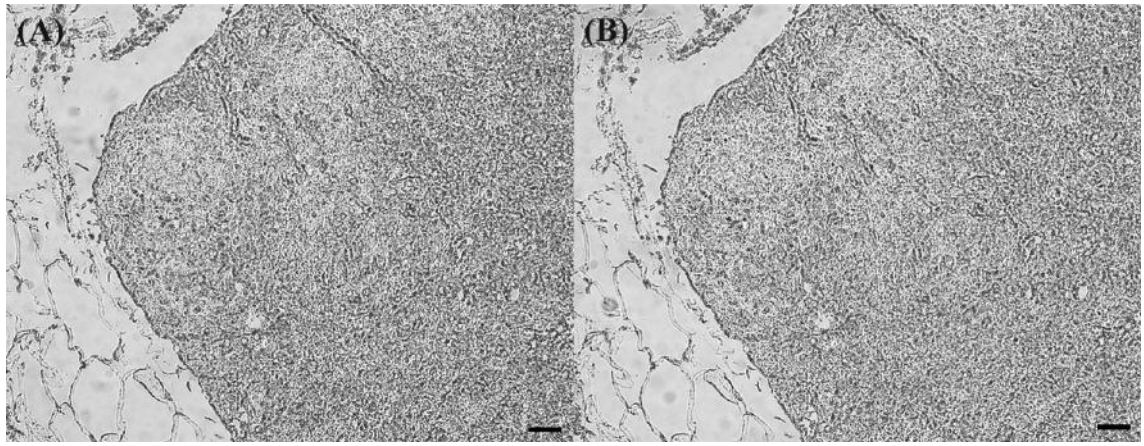

Figure 5. Silver staining of rat lymph node without any QDs showed no trace of silver after 60 min. (A) Before silver staining. (B) After 60 min of silver staining. These results demonstrate that QDs are required for silver staining. Scale bars are 20 μm.

and hydroquinone adsorbs onto its surface. The transfer of electrons from hydroquinone molecules through the nanostructure to adhering silver ions reduces the latter to metallic silver. Reduced silver atoms deposit on the surface and assume the same catalytic role as the original nanostructure by recruiting additional silver atoms onto the surface, effectively amplifying its size until visible under magnification. Because metal sulfides and metal selenides have been previously reported to be effective catalytic surfaces for such silver reduction process,[17] we tested whether distribution of QDs in biological tissues can be conveniently visualized through this silver staining mechanism.

Growth of silver on QDs was directly observed by TEM, as shown in Figure 1B. Although the process is heterogeneous, the overall sizes of QDs were effectively increased. Formation of silver nanoparticles in solution was also discernible by simple visual inspection of the yellow color which resulted immediately upon addition of the silver staining reagents.

We compared the colorimetric response of six different solutions to silver staining, shown in Figure 1C. In contrast to the immediate colorimetric response observed for QD solution, no color change was observed in solutions of phosphate buffered saline (PBS), serum, tissue homogenate, Cd^{2+} ions or polystyrene

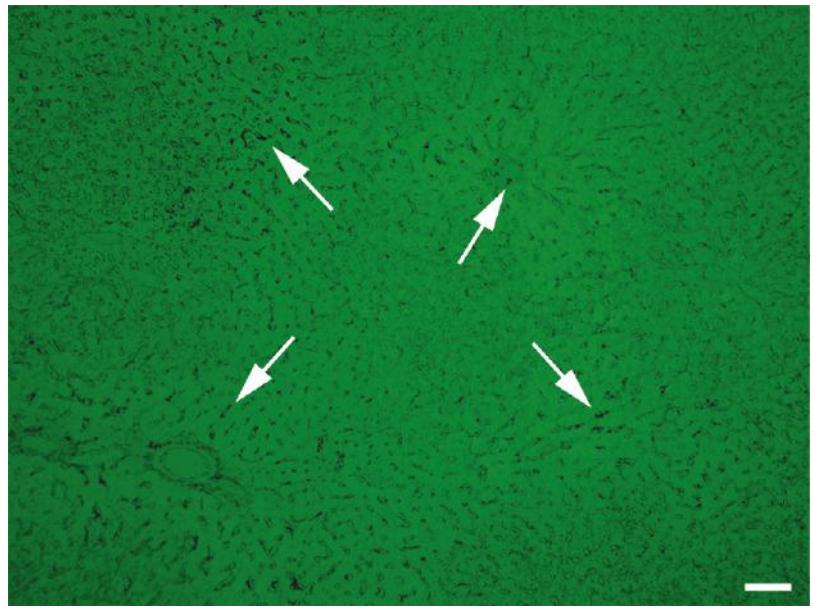

Figure 6. Silver staining of rat liver excised 60 days post-injection with PEG coated QDs. QDs with emission of 558 nm were previously undetectable because of a high background tissue autofluorescence are visualized as dark silver grains. Image taken with Olympus IX71 inverted epifluorescence microscope ($\lambda_{Excitation}$ = 360/40 nm, $\lambda_{Emission}$ = 520 nm long pass). Scale bar is 50 μm.

(PS) beads. The significantly faster kinetics of silver reduction on surfaces of QDs over the other materials tested is important to controlling spontaneous nucleation of silver onto endogenous materials and soluble ions, thereby minimizing non-specific staining on tissues.

This mechanism of silver staining may be applied to identify QDs subjected to significant loss in fluorescence as a result of oxidative quenching by endogenous metabolic pathways. To test this, PAA-ODA coated QDs were exposed to oxidative quenching by hypochlorous acid[8] at molar ratios of 100 to 10000 HOCl molecules per QD. Changes in the photophysical properties of QDs were monitored by UV−vis absorption and photoluminescence. At a molar ratio of 100 HOCl per QD, a detectable decrease in UV−vis absorbance and fluorescence was measured, while the absorbance retained the features of original QDs (Figure 2A,B). Loss of fluorescence was attributed to formation of localized surface defects, which facilitate non-radiative exciton recombination. At a molar ratio of 10000:1, the UV−vis absorbance becomes featureless accompanied by complete fluorescence quenching (Figure 2C,D), indicating significant degradation and partial chemical dissolution of QDs. Following oxidative quenching, both QD solutions were mixed with silver staining solution. In both cases, formation of silver nanoparticles was evident by simple visual inspection and confirmed quantitatively by an absorbance peak at ~430nm (Figure 3).

Next, we explored the use of silver staining to visualize QD distribution within tissue sections. In a typical experiment, FFPE sections were dewaxed, cleaned with deionized water for 30 s, and exposed to aliquots of the silver staining mixture for ~45 to 80 min. This amount of time is longer than the common immunogold-based silver staining method,[12] and depends on the thickness of tissue section, size of QDs, and their surface ligands. Staining was terminated by a second thorough rinse in distilled water. Development took place in a light-covered box to minimize non-specific growth of silver grains caused by the photocatalyzed self-nucleation of silver ions.

Figure 4 compares the distribution of QDs and silver stains within an FFPE section of rat lymph tissue before (Figure 4A) and after staining (Figure 4B). Figure 4A shows the fluorescence image of QDs (emission peak: 600nm, coating: lysine cross-linked mercaptoundecanoic acid, Ly-MUA) from a previous in vivo pharmacokinetic study.[2] Figure 4B shows distribution of the silver stains formed after 50 min of development. The pattern of the stain co-localized with the distribution of QDs, as shown by an overlay in Figure 4C. Isolated QD clusters were stained as discrete, circular silver grains while closely localized QD clusters appeared as agglomerated islands of silver. Several characteristic grains did not co-localize with visible QDs, demonstrating a possible sub-population of non-fluorescing QDs within the tissue. On the other hand, of the image shown, we identified only two clusters of QDs which did not co-localize with silver grains, most likely as a result of poor staining because of diffusional barriers or reagent limitations. Tissues without QDs did not show any dark staining pattern, demonstrating the silver enhancement, with this optimized protocol, will only occur if QDs are located in the tissues (see Figure 5). However, a high background signal on the tissue could be observed if the tissues are incubated with the staining mixture for a long-time (e.g., several hours) because there are biological molecules that can reduce silver ions as well. In our studies, we generally optimize the incubation time to mitigate a large background.

This silver staining technique was also successfully applied in a separate rat liver specimen to identify PEG-QDs with emission peak at 558 nm, which was previously undetectable by fluorescence microscopy because of high levels of background autofluorescence (Figure 6).

CONCLUSION

In conclusion, we present a simple silver staining approach for visualizing a broad range of QDs within histological tissue specimens. This method is fast, sensitive, and easy to perform. More importantly, the mechanism of silver staining is amenable

to QDs of a range of surface compositions, and permits detection of photodegenerate QDs otherwise unaccounted for by fluorescence imaging. As a result, this approach could be applied to cellular labeling studies, to study the extent of photostability of QDs in various tissues, or as a way to conveniently and faithfully retrieve QD distribution patterns in archival histology samples.

ACKNOWLEDGMENT

This work was supported by the Canadian Institute of Health Research, Natural Sciences and Engineering Research Council (NSERC), Canadian Foundation for Innovation, Ontario Innovation Trust. H.C.F. and S.D.P. acknowledge NSERC for a fellowship. We thank Tanya Hauck for some of the tissue samples.

Received for review February 13, 2009. Accepted April 2, 2009.

AC900344A